Model-based compartmental analysis indicates a reduced mobilization of hepatic vitamin A during inflammation in rats[1]

Sin H. Gieng,* Michael H. Green,† Joanne B. Green,† and Francisco J. Rosales[2,§]

Children's Hospital Oakland Research Institute,* Oakland, CA; Department of Nutritional Sciences,† Pennsylvania State University, University Park, PA; and Mead Johnson Nutritionals,§ Evansville, IN

Abstract Vitamin A (VA) kinetics was studied in rats with marginal VA stores before, during, and after inflammation. Rats received orally [11,12-^{3}H(N)]retinol ([^{3}H]VA; day 0), and inflammation was induced on day 21 with lipopolysacchride (LPS) for 3 days (n = 5) or recombinant human interleukin-6 (rhIL-6) for 7 days (n = 5). Both the fraction of [^{3}H]VA and retinol concentrations in plasma were reduced significantly by LPS or rhIL-6. Compartmental analysis using the Windows version of Simulation, Analysis, and Modeling software was applied to group mean data, and non-steady-state models were developed. After absorption, VA kinetics was described by a three-compartment model that included plasma, kidney/interstitium, and liver/carcass. Four mechanisms decreasing plasma retinol were investigated: increased urinary excretion, increased irreversible loss, increased movement into interstitium, and decreased hepatic mobilization. Modeling demonstrated that a 79% reduction in hepatic mobilization of retinol (from 4.3 to 0.9 nmol/h) by 15 h after LPS best accounted for the observed changes in plasma VA kinetics (sum of squares = 9.05×10^{-07}). rhIL-6 caused an earlier reduction (75% by 5.6 h). These models predicted a return to control values by 10 days after inflammation. If prolonged, inflammation-induced hyporetinolemia can render hepatic retinol unavailable to extrahepatic tissues, possibly leading to their impaired function, as observed in VA-deficient children with measles infection.— Gieng, S. H., M. H. Green, J. B. Green, and F. J. Rosales. **Model-based compartmental analysis indicates a reduced mobilization of hepatic vitamin A during inflammation in rats. *J. Lipid Res.* 2007.** 48: **904–913.**

Supplementary key words hyporetinolemia • kinetic analysis • retinol • Windows version of Simulation, Analysis, and Modeling software

Infections such as measles are characterized by a severe inflammatory response, increased production of the inflammatory cytokines, including interleukin-6 (IL-6), and decreased concentrations of circulating retinol (i.e., hyporetinolemia) (1). Measles-induced hyporetinolemia has been associated with increased morbidity and mortality and the development of xerophthalmia in children from areas where vitamin A (VA) may or may not be a public health problem (2, 3). Moreover, supplementation with large doses of VA (200,000 IU of VA on 2 consecutive days) reduced these children's morbidity, mortality, and risk of blindness (4). Although this hyporetinolemia has been well documented and is postulated as mediating measles morbidity and mortality, little is known about the mechanism leading to decreased plasma retinol concentrations or its consequences.

Several hypotheses have been proposed to explain inflammation-induced hyporetinolemia, including decreased intake, malabsorption, direct loss, increased requirement, and impaired utilization (5). The possible underlying mechanisms include the following: *1*) impaired absorption or cleavage of dietary proformed carotenoids or preformed VA (6); *2*) increased utilization of VA subsequent to its immune-potentiating role during infections (7); *3*) increased glomerular filtration followed by an impaired reabsorption in the proximal tubule, leading to retinol and retinol binding protein (RBP) being excreted in urine (8); and *4*) reduced hepatic synthesis of RBP and decreased secretion of retinol into plasma (9, 10). We have shown previously that inflammation induced with lipopolysaccharide (LPS) or recombinant human interleukin-6 (rhIL-6) decreases the availability of RBP and increases the concentrations of hepatic retinol or retinyl esters (9, 11). However, the effect(s) of this decrease in RBP and the increase in hepatic VA on the kinetics and dynamics of

Manuscript received 12 December 2006 and in revised form 17 January 2007.

Published, JLR Papers in Press, January 18, 2007.
DOI 10.1194/jlr.M600528-JLR200

Abbreviations: AIC, Akaike's Information Criterion; fdose, fraction of the oral dose; IL-6, interleukin-6; LPS, lipopolysaccharide; RBP, retinol binding protein; rhIL-6, recombinant human interleukin-6; TMMP, trimethylmethoxyphenyl; VA, vitamin A; [^{3}H]VA, [11,12-^{3}H(N)]retinol; WinSAAM, Windows version of Simulation, Analysis, and Modeling software.

[1] Part of this work was presented at the Federation of American Societies for Experimental Biology 2005, Washington, DC, by S.H.G.

[2] To whom correspondence should be addressed.
e-mail: francisco.rosales@bms.com

whole-body retinol flux during inflammation has not been studied previously.

In previous studies, model-based compartmental analysis has been fruitfully applied to describe and quantify the dynamics of whole-body VA metabolism and to understand the impact of various treatments on VA kinetics (12–17). A major observation from this type of analysis has been the extensive recycling of VA (i.e., retinol and retinyl esters) before it is irreversibly lost (18). Using these techniques, it was determined that the recycling of VA is affected by VA status (i.e., deficiency vs. sufficiency) (19) and by nutritional and chemical stressors, including iron deficiency (20), *N*-(4-hydroxyphenyl)retinamide treatment (21), and 2,3,7,8-tetrachlorodibenzo-*p*-dioxin exposure (22). By comparing model parameters in different physiological, nutritional, or pathological states, the technique provides information on the sites of impact of various treatments. Our objective was to use mathematical modeling and model-based compartmental analysis to assess the potential mechanisms responsible for inflammation-induced hyporetinolemia.

MATERIALS AND METHODS

Materials

Unless noted otherwise, chemical reagents were purchased from EMD Chemicals (Gibbstown, NJ), Fisher Chemicals (Pittsburgh, PA), Mallinckrodt Baker (Phillipsburg, NJ), Pharmco (Brookfield, CT), and Sigma (St. Louis, MO). rhIL-6 was purchased from Austral Biologicals (San Ramon, CA), and LPS derived from *Pseudomonas aeruginosa* was purchased from Calbiochem (San Diego, CA). Osmotic minipumps were purchased from Alzet (Cupertino, CA). Trimethylmethoxyphenyl (TMMP)-retinol was a generous gift from Hoffmann-La Roche (Basel, Switzerland). [11,12-^{3}H(N)]retinol ([^{3}H]VA) was obtained from NEN Life Science Products (lot No. 3354284; Boston, MA). To protect samples from photooxidation, all VA analyses were conducted under fluorescent lights shaded with an ultraviolet light-blocking film (Sydlin, Inc., Lancaster, PA).

Animals and sample collection

Male pathogen-free Sprague-Dawley rats were purchased from Charles River Breeding Laboratories (Kingston, NY). All experimental procedures were approved by the Institutional Animal Care and Use Committee at Pennsylvania State University. All animals were housed with a 12 h light/dark cycle at 22°C and provided diet and water ad libitum.

During kinetic studies, serial blood samples were collected from 2 h to 54 days after [^{3}H]VA administration. Blood was collected from a caudal blood vessel (n = 34–36; 0.25 ml) into heparinized tubes (20 U heparin/ml blood). After centrifugation (Sorvall RT6000B, H-1000B rotor) at 1,300 *g* for 15 min at 4°C, plasma was collected, purged with nitrogen gas, and stored at −80°C until analysis. At the end of each experiment, rats were killed by carbon dioxide asphyxiation. Terminal blood was drawn via cardiac puncture into heparinized syringes. The animals were then perfused with PBS, and livers and carcasses were collected immediately by dissection, blotted, and frozen at −80°C and −20°C, respectively, until analysis.

Pilot experiment

A pilot study was initially conducted to establish parameters to use in the kinetic study, including the adequate oral dose of tracer ([^{3}H]VA), the time for the tracer to equilibrate with body pools of VA, and the time the rats needed to recover from experimentally induced inflammation. At 2 months of age, VA-sufficient rats (n = 4) were given an oral dose of [^{3}H]VA dissolved in 0.29 g of soybean oil (1.44×10^5 Bq/dose) using a polyethylene tube, a 21 gauge needle, and a 1 ml syringe. Twenty-one days later, VA kinetics was perturbed by continuous administration of either LPS (n = 2; 500 μg/kg/day) for 3 days or rhIL-6 (n = 2; 65 μg/kg/day) for 7 days via osmotic minipumps implanted subcutaneously. Sixteen to 19 d later, each rat was euthanized by carbon dioxide asphyxiation, and terminal blood and livers were collected and frozen until analyses.

Kinetic study

Upon arrival, weanling rats (n = 22) were fed 8.02 μmol retinyl palmitate/kg diet for 7 days. They were then fed 2.44 μmol retinyl palmitate/kg diet for the remainder of the study. The first diet was intended to increase their liver stores to ~200 μg (~700 nmol), and the second diet provided the rats with ~14 μg retinol equivalents/day assuming consumption of ~20 g diet/day. These levels of VA were based on estimates from a previous study (23). The diet was made in the laboratory, and its composition (except VA) was based on the American Institute of Nutrition-93 rodent diet formula for growth, pregnancy, and lactation (24).

At 7 weeks of age, 14 rats received an oral dose of [^{3}H]VA in soybean oil (9.3×10^5 Bq/dose) (**Fig. 1**). After equilibration of

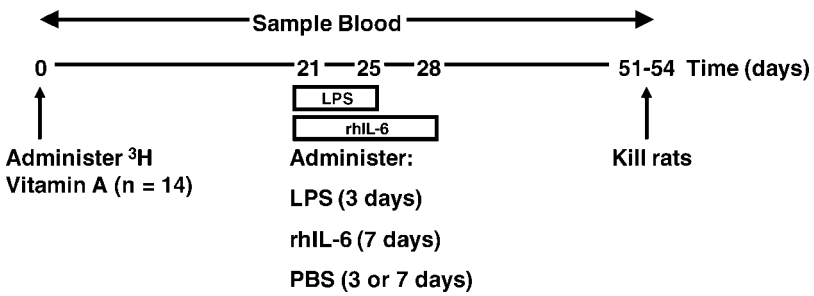

Fig. 1. Experimental design of the main kinetic study. Adult male Sprague-Dawley rats were administered [11,12-^{3}H(N)]retinol ([^{3}H]VA) orally (day 0, n = 14). On day 21, rats were continuously treated with PBS (3 days, n = 2; 7 days, n = 2), lipopolysaccharide (LPS; 3 days, n = 5), or recombinant human interleukin-6 (rhIL-6; 7 days, n = 5). Twenty-six days later (day 54), rats were euthanized and tissues were collected for analyses. Blood samples (n = 34–36; 0.25 ml) were serially collected from 2 h to 54 days. On days 0 and 21, nondosed rats were euthanized to determine hepatic concentrations of vitamin A (VA; n = 4/time).

tracer with whole-body VA pools, inflammation was induced on day 21 with LPS (n = 5; 500 μg/kg/day) for 3 days or rhIL-6 (n = 5; 65 μg/kg/day) for 7 days via osmotic minipumps implanted subcutaneously. PBS was similarly given to controls for 3 days (n = 2) or 7 days (n = 2). At 0 and 21 days, additional rats were euthanized to determine baseline and perturbation liver VA concentrations (n = 4/day). We selected LPS and rhIL-6 at these doses because in our previous experiments (9, 11) we demonstrated that these doses induced inflammation without septicemia or renal failure, and they allowed us to examine the effects of the acute-phase response of inflammation on the distribution of VA and RBP in various tissues (9, 11). Additionally, rhIL-6 induced and maintained the acute-phase response of inflammation for up to 7 days without causing metabolic alterations or reducing food intake (11).

Plasma and tissue analyses

For analysis of tritium in plasma samples, retinol was extracted into hexane as described previously (11, 25), solvent was removed under a stream of nitrogen, and 5 ml of scintillation solution (Betamax ES; ICN Biomedicals) was added to each liquid scintillation vial. Tritium content of each sample was determined using a Beckman Liquid Scintillation System (LS 3801). Each sample was counted to a 2σ error level of 1% after a counting efficiency calibration was performed using a quench curve, and dpm was determined.

Retinol concentrations in plasma for 17 of the samples collected over the experimental period for each rat were determined by HPLC (Hewlett-Packard 1100) using TMMP-retinol as an internal standard (25) after extraction with hexane. The reverse-phase system included a Zorbax Eclipse XDB-C8 (5 μm, 4.6 × 150 mm) with a C8 guard column (Agilent Technologies, Wilmington, DE) and a multiple wavelength ultraviolet light detector. Retinol was detected at 325 nm.

Frozen livers were lyophilized and analyzed for VA mass and/or radioactivity. Aliquots of freeze-dried livers were saponified using a modified method described previously (16). Triplicate weighed aliquots of liver (~0.15 g) were combined with 1.0 ml of ethanol containing 0.1% pyrogallol as an antioxidant. TMMP-retinol (internal standard) and 0.5 ml of 60% aqueous KOH were then added. Samples were purged with nitrogen and allowed to incubate at 60°C for 60 min. After saponification, the lipid fraction was extracted three times using 5 ml of hexane containing 5 μg butylated hydroxytoluene/ml and 1 ml of distilled water. A portion of the extract was dried under a stream of nitrogen in liquid scintillation vials, 10 ml of scintillation solution was added, and its radioactivity was determined. A separate aliquot of the extract was dried under nitrogen, reconstituted in methanol, and analyzed for retinol by HPLC as described above.

Kinetic analysis

Model-based compartmental analysis was performed to develop the simplest compartmental model compatible with tracer and tracee data for plasma, liver, and carcass. The Windows version of the Simulation, Analysis, and Modeling software (WinSAAM) (26) was used for this purpose. First, the fraction of the oral dose (fdose) in plasma at each time was estimated as dpm/ml in plasma divided by administered dpm/estimated plasma volume (ml). Plasma volume was estimated from body weight on day 25 of the study (g) × 0.038 ml plasma/g body weight (27).

To determine a model of VA metabolism before the perturbation caused by inflammation, normalized plasma data before 21 days were used. Values in each group (PBS, LPS, and rhIL-6) were averaged to develop a preperturbation control model. Because the tracer was administered orally, an absorption/processing model first needed to be developed to account for this (28). After the absorption model was developed, a three-compartment model was developed, similar to a previously published conceptual model (23). Fractional transfer coefficients [$L(I,J)$s, or the fraction of compartment J that is transferred to compartment I per unit time] were then determined.

To account for the administration of the perturbing doses of PBS, LPS, or rhIL-6, a time interrupt was introduced into plasma data at day 21. Moreover, a second independent variable, theta, was introduced to allow for the adjustment of parameters during the perturbation. Fractional transfer coefficients before day 21 were fixed. After day 21, the fractional transfer coefficients were adjusted one at a time to find the minimal change necessary to fit the observed data obtained after the perturbations.

The LPS data were used to develop an initial model. Four potential causes explaining LPS-induced hyporetinolemia were investigated (increased urinary excretion, increased irreversible loss, increased movement into interstitial fluid, and decreased hepatic mobilization of retinol) by adjustment of kinetic parameters believed to represent these changes. Best-fit models were determined based on a statistically close fit of the model to the observed data (sum of squares). A two-part difference equation was used to represent the changes in one parameter. This equation used the second independent variable feature of WinSAAM to represent the time since the beginning of the perturbations. Changes to parameters in the model were as follows: *1*) increased urinary excretion, added L(10,6) (see Table 2, Fig. 5 below); *2*) increased irreversible loss, adjusted L(10,7); *3*) increased movement into interstitial fluid, adjusted L(6,5) and L(5,6); and *4*) decreased hepatic mobilization of retinol, adjusted L(5,7).

Statistical analysis

Descriptive data are presented as group means ± SD. Data were compared statistically using a Student's unpaired *t*-test in Microsoft Excel (2003 version) with $P \leq 0.05$ considered significant. The data for each treatment group (PBS, LPS, and rhIL-6) were averaged for the kinetic analyses using WinSAAM (26). Because compartmental modeling was done using group mean data at each time, it was not possible to compare kinetic parameters statistically between groups. With the present study design (preperturbation, perturbation, and postperturbation portions of the model), each group of rats served as its own control (i.e., data before the perturbation). For weighting purposes, model development based on observed data was set at a fractional standard deviation of 5% (SD/mean). The weighted sum of squares represents the sum of the squared differences between observed and model-predicted data points and was used to evaluate the closeness of the predicted model to the observed data. Akaike's Information Criterion (AIC) was calculated for each model to determine which had the lowest number (the best fit) for the observed data (29).

RESULTS

Pilot experiment

In the pilot study, determination of labeled retinol in the plasma of rats indicated the successful administration and absorption of the tracer dose. Both LPS- and rhIL-6-treated rats showed similar tracer response profiles in plasma up to ~21 days. When the inflammation-inducing agents were administered beginning on day 21, there was an ~63% reduction in plasma tracer levels over 6 days in the LPS-treated rats, whereas rhIL-6-treated rats had an

~89% reduction over 10 days. Tracer in plasma for both treatment groups returned to preperturbation levels after inflammation. However, it was apparent that the post-perturbation time after rhIL-6 treatment was not long enough to clearly see the postinflammation and terminal data. Therefore, the subsequent experiment was extended an additional 2 weeks.

Kinetic study: dynamics of retinol (tracee)

Hyporetinolemia was observed in rats treat with LPS (−42% plasma retinol concentrations relative to controls; $P = 0.0004$) or rhIL-6 (−57% plasma retinol concentrations relative to controls; $P = 0.0002$). Note that retinol concentrations in PBS controls decreased by ~16% at 3 days after surgery ($P = 0.14$) (**Fig. 2**). The fraction of [^{3}H]VA in plasma decreased during inflammation and returned to control levels after 6 days in LPS-treated rats and after 16 days in rhIL-6-treated rats. In contrast to effects related to inflammation, plasma concentrations of retinol before and after perturbation were the same within each group, as indicated by the slope of the line describing this change ($P > 0.20$).

Dynamics of [^{3}H]VA (tracer)

After calculating the fdose in plasma for each rat at each time point, the arithmetic means at each time point were calculated for each treatment group. These data were plotted on semilogarithmic graphs. For each group, there was a rapid initial increase in tracer that peaked at 7.1–8.4% of the dose by 6 h. The fdose declined thereafter and reached a terminal slope by ~10 days after oral tracer administration. This terminal slope remained unchanged until day 21, at which point each rat was perturbed with PBS, LPS, or rhIL-6. In PBS control rats, plasma tracer was reduced slightly for the duration of the treatment period (7 days). In rats treated with LPS, there was a rapid reduction in plasma tracer that reached a nadir by ~2 days and then increased to preperturbation levels by 6 days. In rats treated with rhIL-6, there was an even more rapid and larger reduction than in LPS-treated rats. This reduction in tracer persisted for ~8 days, when it started to return to preperturbation levels. After the perturbation, the terminal slope was less shallow compared with the preperturbation terminal slope.

Specific activity of tracer and tracee

The specific activity of tracer in plasma (the ratio of the fdose to the concentration of plasma retinol) is shown in **Fig. 3**. Before inflammation, changes in plasma retinol specific activity were similar for the three groups. The specific activity in both LPS- and rhIL-6-treated rats decreased at the beginning of inflammation and returned to PBS control levels after inflammation.

Kinetic analysis: absorption and processing of the tracer

Compartmental analysis of group mean data using the WinSAAM computer program was applied to develop steady-state models of VA kinetics based on data for the

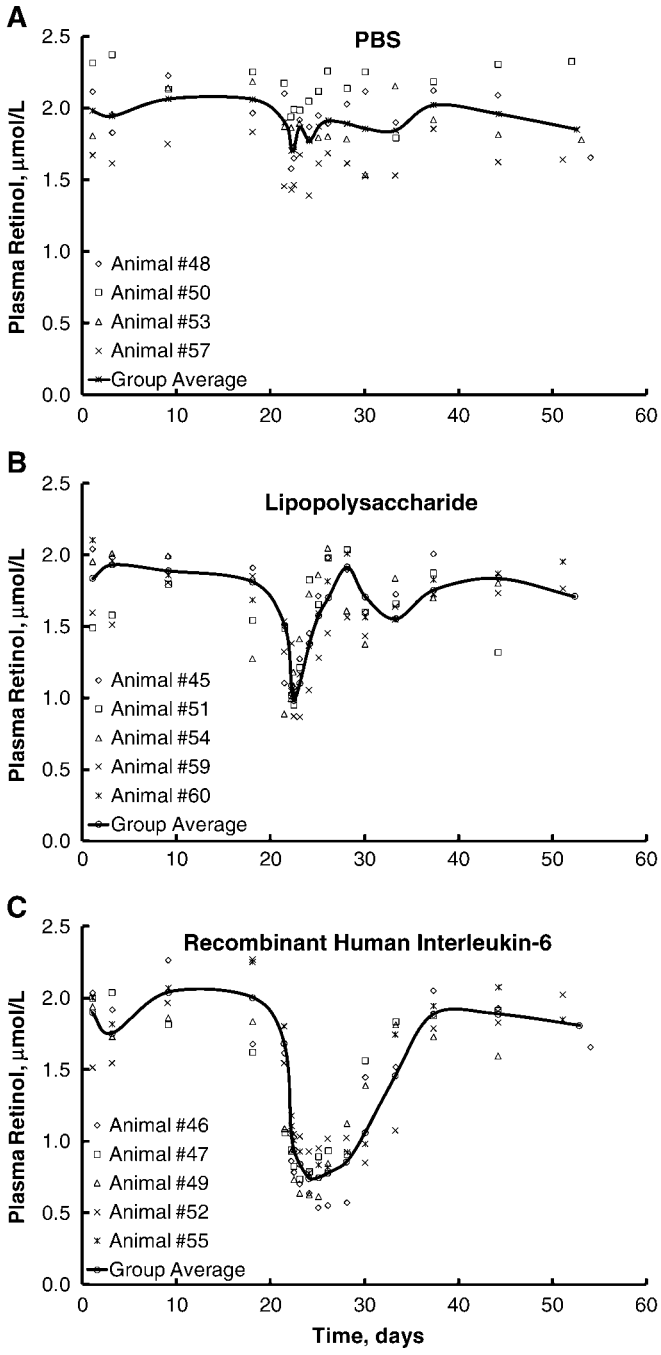

Fig. 2. Plasma retinol concentrations in PBS-, LPS-, and rhIL-6-treated rats. A: PBS, control. B: LPS. C: rhIL-6. Numbers represent rat identification numbers. Curves represent smooth lines through averaged data at each time point.

first 21 days (**Fig. 4**). A four-compartment preabsorption and chylomicron-processing model was necessary to follow the behavior of the orally administered tracer (Fig. 4, open circles). This is represented in the initial increase in plasma tracer in the first 6 h after oral dosing. The radioactive tracer entered the system through compartment 1, labeled with the asterisk. After moving into compartment 2, a fraction of the tracer was irreversibly lost from the system. The remaining fraction entered compartment 3 and

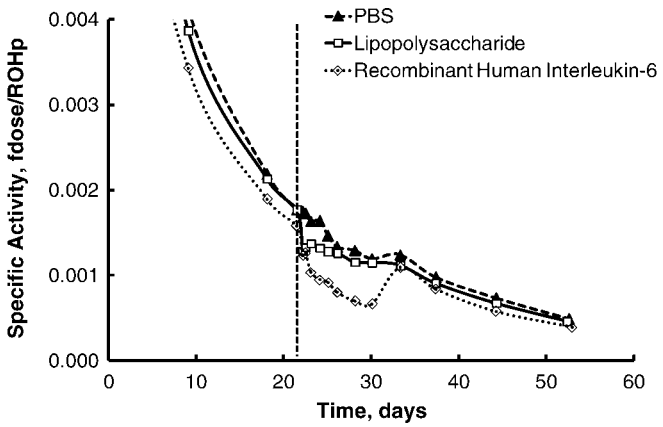

Fig. 3. Plasma retinol specific activity in PBS-, LPS-, and rhIL-6-treated rats. Specific activity was calculated as the fraction of the oral dose (fdose) divided by the plasma retinol concentration (ROHp) at each time point. Curves represent smooth lines through data averaged at each time point. The vertical dashed line represents the time at which PBS, LPS, or rhIL-6 was initially administered.

represents the percentage of the dose absorbed (~23–27%). Compartment 3 is a delay built into the model to represent the biological processes of chylomicron and hepatic retinyl ester metabolism. This processing or delay lasted ~1 h. After this delay, the tracer entered compartment 4 and then immediately entered the postabsorption/processing plasma pool (compartment 5).

Kinetic analysis: three-compartment model (preperturbation)

The preperturbation models were based on data from the first 21 days of the experiment. Once the tracer was absorbed, processed, and entered the plasma, the kinetics of whole-body VA was analyzed using a three-compartment model (Fig. 4, closed circles). These three compartments were represented largely by plasma (compartment 5), kidneys/interstitial fluid (compartment 6; fast turning-over pool), and liver and carcass (compartment 7; slow turning-over pool), as hypothesized by two of the authors (30). Postabsorption irreversible loss or utilization (e.g., through catabolism and metabolism) occurred in the slow turning-over pool and thus was represented by movement into the irreversible loss pool (compartment 10). To estimate compartment masses and transfer rates, the calculated plasma retinol pool size was entered into the model. The parameters estimated for the preperturbation model's compartment masses [M(I)], transfer rates [R(I,J)], plasma fractional catabolic rates, and system disposal rates [R(10,7)] are listed in **Table 1**.

The predicted model clearly fits the preperturbation data but not the remaining data for each treatment group

TABLE 1. Compartment masses, transfer rates, plasma fractional catabolic rates, and absorption efficiencies predicted by the absorption and three-compartment model of vitamin A metabolism for PBS-, LPS-, and rhIL-6-treated rats before perturbation

	Treatment Groups		
Parameter	PBS	LPS	rhIL-6
M(1), nmol	14.34	6.53	7.53
M(2), nmol	3.45	1.49	2.04
M(3), nmol	59.73	1.33	1.02
M(4), nmol	2.44	2.01	5.27
M(5), nmol	39.12	35.44	33.77
M(6), nmol	64.27	53.16	50.96
M(7), nmol	370.22	324.29	431.03
R(2,1), nmol/day	149.75	139.08	148.19
R(3,2), nmol/day	36.06	31.79	40.11
R(4,3), nmol/day	36.06	31.79	40.11
R(5,4), nmol/day	36.06	31.79	40.11
R(10,2), nmol/day	113.70	107.29	108.08
R(6,5), nmol/day	516.02	425.29	430.81
R(5,6), nmol/day	516.02	425.29	430.81
R(7,5), nmol/day	155.22	125.30	143.44
R(5,7), nmol/day	119.17	93.51	103.33
R(10,7), nmol/day	36.06	31.79	40.11
Plasma fractional catabolic rate, day^{-1}	0.92	0.90	1.19
Absorption, %	24.10	22.90	27.10

LPS, lipopolysaccharide; M, mass; R, transfer rate; rhIL-6, recombinant human interleukin-6.

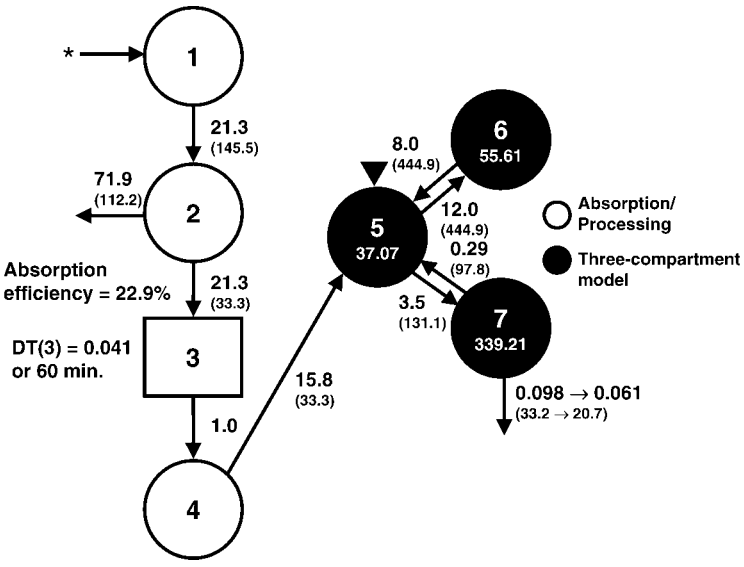

Fig. 4. Working compartmental model developed to fit tracer data from plasma for LPS-treated rats. Circles represent compartments, and arrows represent adjustable model parameters {fractional transfer coefficients [L(I,J)], or the fraction of compartment J's tracer transferred to compartment I each day}. Numbers in parentheses represent fractional transfer rates [R(I,J)] or the nmol of J's tracee transferred to compartment I each day. Numbers in compartments 5, 6, and 7 represent compartment masses [M(I)] or the nmol of tracee in each compartment. The rectangle (3) represents a delay element included to explain chylomicron and hepatic VA processing. Tracer was administered into compartment 1 (asterisk), and samples were taken from the plasma or compartment 5 (triangle). DT, delay time.

(**Fig. 5A–D**). After the perturbation, the terminal slope was slightly more shallow compared with the preperturbation terminal slope. That is, the predicted amount of tracee irreversibly leaving the system (i.e., disposal rate) decreased in response to the surgery and implantation of the pump, from 36.1 to 17.1 nmol/day in the PBS group, from 31.8 to 27.2 nmol/day in the LPS group, and from 42.3 to 20.5 nmol/day in the rhIL-6 group. Because this reduction occurred similarly in control rats and rats treated with LPS or rhIL-6, it suggested an on or off response independent of the relative severity of the inflammatory stimulus.

Kinetic analysis: potential causes of hyporetinolemia

To model urinary excretion, irreversible loss was added from the fast turning-over extravascular pool [compartment 6; L(10,6) (Fig. 5A)]. Even if the model was adjusted so that all VA entering the fast turning-over pool was irreversibly excreted, this did not adequately fit the observed VA kinetics and dynamics. The same was true when an increase in irreversible loss from the slow turning-over pool was modeled (Fig. 5B). It may also have been possible that VA moved into interstitial fluid during inflammation. To model this phenomenon, a temporary net input of VA into the fast turning-over extravascular pool was applied (i.e., increased movement of VA out of the blood into the fast turning-over pool and/or decreased movement of VA out of the fast turning-over pool into blood) (Fig. 5C). This model fit better the observed plasma VA kinetics and dynamics than the previous two models. However, biologically, this model of inflammation-induced hyporetinolemia was unlikely, because an elimination of irreversible loss of VA is required for this model to fit the observed data. In contrast, a 79% reduced mobilization of hepatic retinol (from 4.3 to 0.9 nmol/h) by 15 h best accounted for the observed changes in plasma VA kinetics in the LPS group (Fig. 5D), which was modeled using a two-part multiexponential difference equation. Model parameter changes for these potential causes are represented in **Table 2**. Changes to parameters in the model were as follows: increased urinary excretion, add L(10,6); increased irreversible loss, adjust L(10,7); increased movement into interstitial fluid, adjust L(6,5) and L(5,6); and decreased hepatic mobilization of retinol, adjust L(5,7). The sum of squares and the AIC number indicated that the model that best fit the data was decreased hepatic mobilization.

The model of decreased hepatic mobilization of retinol was then applied to kinetic data from rhIL-6-perturbed rats. Similar to LPS treatment, the adjustment of one parameter provided an adequate fit of the model to the observed changes in tracer (**Fig. 6**). At the beginning of the perturbation, an immediate reduction in L(5,7) accounted for the first 8 days since the perturbation. This parameter decreased by ~75% (from 0.24 to 0.06 pools/day) with rhIL-6 treatment compared with a reduction of 76% (from 0.29 to 0.07 pools/day) with LPS treatment (**Fig. 7**). The maximum reduction caused by LPS took ~17.5 h versus ~5 h with rhIL-6 treatment. After 8 days, the increasing portion of the exponential equation was applied to account for the increase in observed plasma

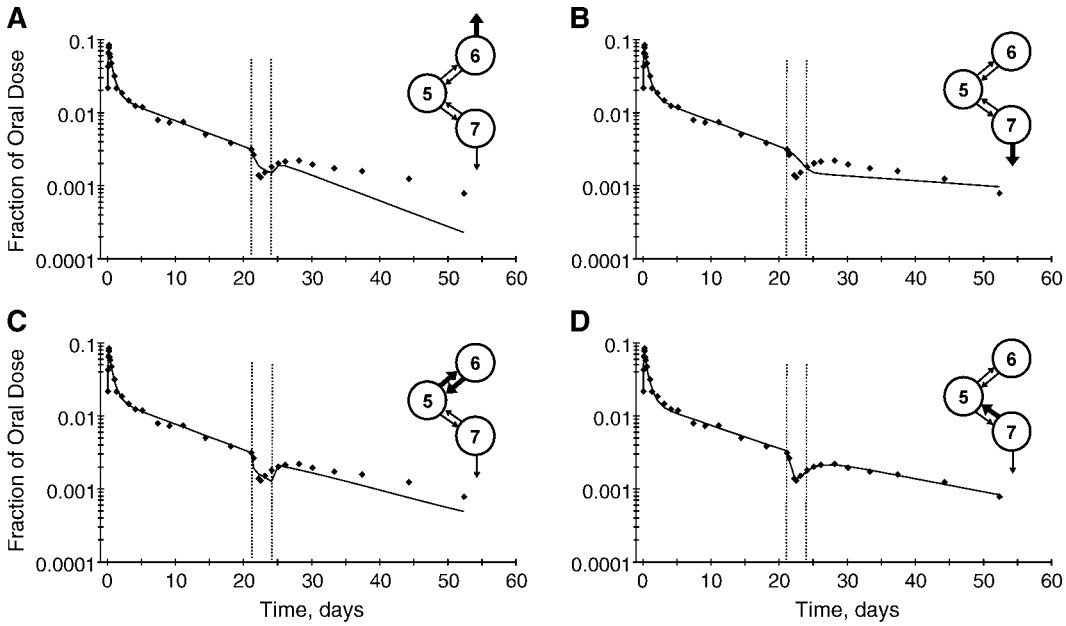

Fig. 5. Model-predicted curves of urinary excretion (A), increased irreversible loss (B), increased movement into interstitial fluid (C), and decreased hepatic mobilization (D) of VA in LPS-treated rats. Diamonds represent observed data points (mean of five rats), and solid lines represent the model-predicted curve. The vertical dotted lines represent the duration of LPS treatment (3 days). Circles represent kinetically distinct compartments (5, plasma; 6, kidney/interstitium; 7, liver/carcass). The thin arrows represent unaltered parameters, and the thick arrows represent added or adjusted parameters.

TABLE 2. Sum of squares and changes in parameters to model increased urinary excretion, increased irreversible loss, increased movement into interstitial fluid, and decreased hepatic mobilization in LPS-treated rats

Mechanism	Parameter	Preperturbation Value	Perturbation Value (day 0)	Postperturbation Value (day 3)	Sum of Squares (Akaike's Information Criterion)
Increased urinary excretion	L(10,6)	00.000	1.769	00.000	1.07×10^{-5} (−381)
	L(10,7)	00.098	0.000	00.000	
Increased irreversible loss	L(10,7)	00.098	0.298	00.018	1.41×10^{-5} (−375)
Increased movement into interstitial fluid	L(5,6)	8.000	0.000	5.036	4.55×10^{-6} (−404)
	L(6,5)	12.000	2.496	37.265	
	L(10,7)	00.098	0.000	00.000	
Decreased hepatic mobilization	L(5,7)	00.288	0.288 × function[a]		1.12×10^{-6} (−450)
	L(10,7)	00.098	0.084	00.084	

[a] G(41) = (K(11) × EXP(−P(1) × TH) + K(12) × (2− (P(4) × (EXP(−P(2) × TH))) −EXP(−P(3) × TH))). In this equation, 41 is an arbitrary name; K indicates intercepts (exponential constants), P indicates slopes (exponential coefficients), T is time (days) since the administration of the tracer, and TH (theta) is a second independent variable representing time (days) since osmotic pump implantation. K(11) = 1.145, K(12) = 0.855, P(1) = 3.335, P(2) = 0.405, P(3) = 0.040, P(4) = 1.169.

tracer. This increase occurred at a slightly faster rate in the rhIL-6 model compared with the rate predicted by the LPS model.

DISCUSSION

The association between infections and hyporetinolemia has been well documented in both clinical and nonclinical studies. However, these studies have had difficulty assessing which is the prime driver because of the close interaction between VA deficiency and infection-induced inflammation. Even clinical studies, in which serial measurements of plasma retinol or urinary RBP have been used to monitor the effect of infection-induced inflammation, have not clearly determined the cause and consequences of hyporetinolemia (31, 32). Experimental studies in animals have shown without exception that plasma retinol can be reduced by a variety of immune stressors ranging from viral infections and turpentine injections to prolonged immobilization (32–36). These studies have suggested various mechanisms, including a decreased secretion of liver RBP (33, 34), a reduced secretion of liver Transthyretin (35), and an increased utilization of plasma retinol (33, 36, 37). However, these studies have not been able to answer questions about what, where, and how hyporetinolemia occurs during inflammation. Even our own studies have been limited by providing a cross-sectional perspective of the changes in plasma retinol among tissues during inflammation induced with LPS or rhIL-6 (9, 11). Because of this limitation, we developed a kinetic study using labeled VA and mathematical modeling using WinSAAM.

In the kinetic study, rats received sufficient VA in the diet to maintain growth and other normal functions yet avoided the accumulation of total whole-body VA stores, as described previously (23). The absorption of tracer was estimated to range from 23% to 27%, lower than expected. Once the tracer was absorbed, the calculated time for enterocyte and hepatic processing of chylomicrons before it was secreted into plasma as the RBP-retinol complex averaged ~40.2 min, and four kinetically different compart-

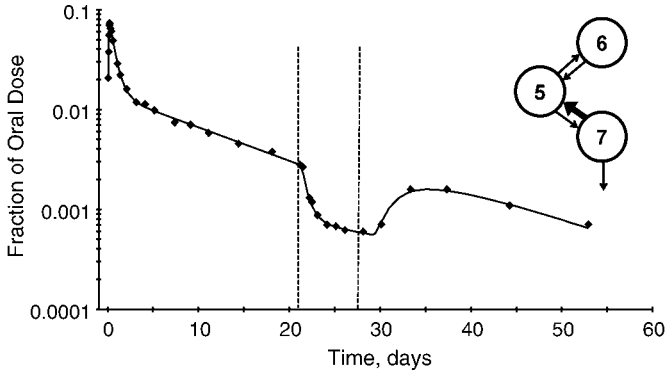

Fig. 6. Semilogarithmic plot of the model-predicted values of VA kinetics before, during, and after rhIL-6-induced hyporetinolemia. Diamonds represent observed data points (mean of five rats), and the solid line represents the best-fit calculated model. The thick arrow represents the adjusted parameter. Time bounded by the vertical dotted lines represents the duration of treatment.

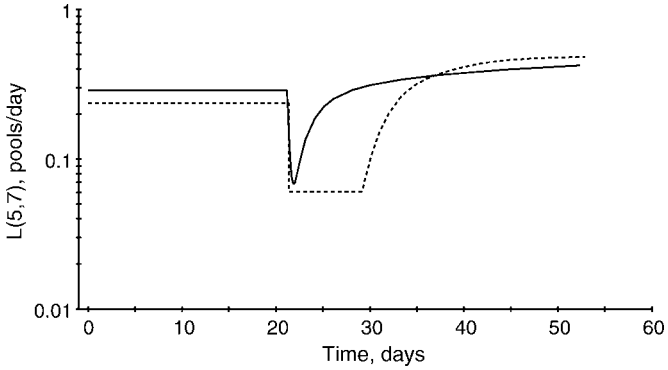

Fig. 7. Model-predicted changes in fractional transfer coefficients over time in LPS- and rhIL-6-treated rats. The solid line represents the predicted change in the fraction of compartment 7 transferred to compartment 5 per day over time in LPS-treated rats. The dashed line represents the predicted change for rhIL-6-treated rats. Compartment numbers are shown in the model in Fig. 4. The multiexponential difference equation for the model of LPS treatment is given in Table 2. The equation for the model of rhIL-6 treatment is G(41) = (K(11) × EXP(−P(1) × TH) + (K(12) × (2 − (P(4) × ((EXP(−P(2) × TH × TH)))) − EXP(−P(3) × TH × TH)))). K(11) = 2 − 1/P(4), K(12) = 1/P(4), P(1) = 1.895, P(2) = 0.00717, P(3) = 0.0406, P(4) = 0.981. TH, theta.

ments were necessary to model this process (Fig. 4), as shown previously (12). Once the tracer entered the plasma, VA kinetics fit a three-compartment model proposed previously (23). In this model (Fig. 4), the central compartment represents plasma retinol bound to RBP- Transthyretin. Although in all animals, tracer had equilibrated with body pools of VA within 10 days after dose administration (Fig. 3A), inflammation was not induced until 21 days to ensure that the dose was highly equilibrated with whole-body pools; then, a control model could be identified. As expected, the parameters representing the preperturbation models for PBS, LPS, and rhIL-6 treatments were similar, because at this point all animals had been treated similarly. Irreversible utilization of VA averaged 36 nmol/day, which was greater than the 27 nmol/day that we estimated rats were consuming, suggesting that these animals were in a negative VA balance (e.g., marginal VA deficiency).

Whole-body VA metabolism was perturbed by surgery (implantation of osmotic minipumps) and then continuous administration of LPS or rhIL-6. The reduction of plasma retinol in PBS control rats was likely attributable to the surgery and implantation of the minipump and was self-limiting and not as substantial as that caused by either LPS or rhIL-6 (Fig. 2). It is interesting that although the duration of LPS treatment was 3 days, the plasma retinol nadir occurred after ~1 day of treatment and then increased rapidly thereafter. In contrast, 7 days of rhIL-6 treatment caused a large reduction in plasma retinol concentration that was sustained to 10 days (3 days beyond the end of treatment) before increasing rapidly. These differences reflected the tolerance to endotoxin induced by repeated or continuous LPS dosing (38) and confirmed the appropriateness of using rhIL-6 to maintain the acute-phase response of inflammation in a model of prolonged hyporetinolemia (11). It is noteworthy that a long-lasting effect of IL-6 in inducing hyporetinolemia has been observed in clinical studies of infections caused by respiratory syncytial virus or measles virus (39, 40). Plasma retinol concentrations before and after hyporetinolemia were not significantly different in either of the treatment groups, suggesting that plasma retinol rebounds from inflammation-induced hyporetinolemia when the inflammatory stimulus is no longer present. In this regard, the study design allowed for the preperturbation and postperturbation comparison within each group.

Similarly, plasma tracer concentrations were affected more by LPS or rhIL-6 treatments than by surgery. Mathematical modeling using WinSAAM revealed that the effect of inflammation was acute and transitory. Although the reductions in plasma tracer paralleled the observed hyporetinolemia, the specific activity (the ratio of tracer to tracee) decreased during the perturbation with LPS or rhIL-6 (Fig. 3). This observation has significant implications for the use of a stable isotope dilution technique to measure VA status (28): if inflammation reduces plasma retinol specific activity, the stable isotope dilution technique will be less accurate.

As indicated above, several mechanisms have been proposed to explain inflammation-induced hyporetinolemia. These include an increased catabolism of VA, an increased transcapillary escape rate, and an increased urinary excretion of retinol (41). To examine these possibilities, we used the mean observed data from LPS-treated rats, because the shape of the tracer curve during the perturbation was less complex. The approach was to determine the smallest necessary change in the model that would account for the observed reduction in plasma tracer and the hyporetinolemia. Four possible models and their associated alteration(s) in parameters were tested (Table 2). The model based on a reduction in the mobilization of retinol from the liver into plasma best fit statistically the observed data (Fig. 5–7, Table 2).

The calculated reduced mobilization was based on a user-defined two-component multiexponential difference equation (Fig. 7). The first part of the equation describes the decrease in the parameter, and the second part represents the increase. The concept and basis for this equation are from a kinetic analysis performed previously (12), and an exponential function was chosen, because the components might have biological meaning. From a biological perspective, hyporetinolemia caused by a decreased hepatic mobilization of VA coincides with our previous findings of a decrease in both protein and mRNA levels of hepatic RBP and the accumulation of retinol and retinyl esters in the liver in response to LPS or rhIL-6 (9, 11). The prolonged hyporetinolemia caused by continuous rhIL-6 infusion was modeled by prolonging the reduction in the rate of mobilization of VA from the liver into plasma. Compared with LPS treatment, rhIL-6 caused a similar but earlier reduction in the rate of mobilization (−79% by 15 h for LPS vs. −75% by 5.6 h for IL-6). This reduction was maintained for 8 days before retinol concentrations increased to preperturbation levels in a manner similar to the modeled increase in LPS-treated rats (Fig. 7). This corroborates the concept that the effect of LPS on VA metabolism is through its induction of IL-6 synthesis by various immune cells, hence LPS's delayed onset in the reduction rate of mobilization. Subsequently, IL-6 presumably affects the VA system by decreasing hepatic RBP production (11).

In our previous experiments with LPS, we observed a decrease in food intake, which was associated with a mild and limiting reduction in plasma retinol (9). In the rhIL-6 model (11), we found that the continuous administration of rhIL-6 for 7 days did not affect food intake significantly. In the present experiments, we observed that LPS and rhIL-6 decreased plasma retinol (Fig. 2), and in both cases the compartmental analysis predicted a reduced mobilization in hepatic retinol (Fig. 7). These results suggest that regardless of changes in food intake (LPS-induced anorexia vs. rhIL-6's no effect on food intake), there was an accumulation of VA in the liver.

In contrast, the increased irreversible utilization and urinary excretion models were inadequate to describe tracer kinetics during the perturbation (Fig. 5, Table 2). It was impossible to account for the dramatic decrease in plasma retinol and its tracer by altering the parameters that represented these changes or to adequately increase plasma

tracer concentrations once the perturbation was complete. For these postulated mechanisms, both the time (initiation, termination, and duration) and magnitude of the parameters were altered to attempt to account for the observed changes; however, these modifications did not improve the fit of the observed to the calculated data (Fig. 5). Comparatively, the hypothesis of increased movement into interstitial fluid provided a closer fit to the observed data (Fig. 5). Here, the size of the pool of VA in the fast turning-over extravascular compartment may have provided a site where VA could transiently move during inflammation, possibly as a result of an associated increase in vascular permeability. If this were the case, however, we would likely also have observed decreases in other similarly sized blood constituents in response to inflammation. Nonetheless, this model did not perfectly fit the observed data and therefore was judged not to be a major contributor to inflammation-induced hyporetinolemia (Table 2; AIC number −404 vs. −450 for decreased hepatic mobilization).

In summary, these findings and their interpretation indicate that inflammation-induced hyporetinolemia can be caused by trauma (i.e., surgery) or by bacterial or viral infections (i.e., LPS or rhIL-6). The duration and extent of the hyporetinolemia depend on the type of immune stressor. Based on our data, we conclude that the most likely underlying mechanism is a reduced synthesis of hepatic RBP (9, 11). Consequently, there is a reduced mobilization or an accumulation of hepatic VA, in part attributable to a reduced recycling of retinol from liver stellate cell retinyl ester stores back into plasma and from impairing the hepatic secretion of recently absorbed dietary VA. Both hyporetinolemia and the accumulation of hepatic VA reduce the availability of VA to extrahepatic tissues, especially those that depend on retinol bound to RBP. In this regard, these findings help to clarify the severity of measles infection and its amelioration with large doses of VA (i.e., 200,000 IU/day on 2 consecutive days) in VA-deficient children.

This work is part of a doctoral thesis by S.H.G. and was supported by a grant from the National Institutes of Health, National Institute of Diabetes and Digestive and Kidney Diseases (RO3 DK-062166 to F.J.R.).

REFERENCES

1. Hussey, G. D., and M. Klein. 1990. A randomized, controlled trial of vitamin A in children with severe measles. *N. Engl. J. Med.* **323:** 160–164.
2. Butler, J. C., P. L. Havens, A. L. Sowell, D. L. Huff, D. E. Peterson, S. E. Day, M. J. Chusid, R. A. Bennin, R. Circo, and J. P. Davis. 1993. Measles severity and serum retinol (vitamin A) concentration among children in the United States. *Pediatrics.* **91:** 1176–1181.
3. Phillips, R. S., C. O. Enwonwu, S. Okolo, and A. Hassan. 2004. Metabolic effects of acute measles in chronically malnourished Nigerian children. *J. Nutr. Biochem.* **15:** 281–288.
4. Barclay, A. J., A. Foster, and A. Sommer. 1987. Vitamin A supplements and mortality related to measles: a randomised clinical trial. *Br. Med. J. (Clin. Res. Ed.).* **294:** 294–296.
5. Stephensen, C. B. 2001. Vitamin A, infection, and immune function. *Annu. Rev. Nutr.* **21:** 167–192.
6. Homnick, D. N., C. R. Spillers, S. R. Cox, J. H. Cox, L. A. Yelton, M. J. DeLoof, L. K. Oliver, and T. V. Ringer. 1995. Single- and multiple-dose-response relationships of beta-carotene in cystic fibrosis. *J. Pediatr.* **127:** 491–494.
7. Ross, A. C., and C. B. Stephensen. 1996. Vitamin A and retinoids in antiviral responses. *FASEB J.* **10:** 979–985.
8. Stephensen, C. B., J. O. Alvarez, J. Kohatsu, R. Hardmeier, J. I. Kennedy, Jr., and R. B. Gammon, Jr. 1994. Vitamin A is excreted in the urine during acute infection. *Am. J. Clin. Nutr.* **60:** 388–392.
9. Rosales, F. J., S. J. Ritter, R. Zolfaghari, J. E. Smith, and A. C. Ross. 1996. Effects of acute inflammation on plasma retinol, retinol-binding protein, and its mRNA in the liver and kidneys of vitamin A-sufficient rats. *J. Lipid Res.* **37:** 962–971.
10. Aldred, A. R., and G. Schreiber. 1993. The negative acute phase proteins. *In* Acute Phase Proteins: Molecular Biology, Biochemistry, and Clinical Applications. A. Mackiewicz, I. Kushner, and H. Baumann, editors. CRC Press, Boca Raton, FL. 21–37.
11. Gieng, S. H., J. Raila, and F. J. Rosales. 2005. Accumulation of retinol in the liver after prolonged hyporetinolemia in the vitamin A-sufficient rat. *J. Lipid Res.* **46:** 641–649.
12. von Reinersdorff, D., M. H. Green, and J. B. Green. 1998. Development of a compartmental model describing the dynamics of vitamin A metabolism in men. *Adv. Exp. Med. Biol.* **445:** 207–223.
13. Green, M. H., L. Uhl, and J. B. Green. 1985. A multicompartmental model of vitamin A kinetics in rats with marginal liver vitamin A stores. *J. Lipid Res.* **26:** 806–818.
14. Green, M. H., and J. B. Green. 1996. Quantitative and conceptual contributions of mathematical modeling to current views on vitamin A metabolism, biochemistry, and nutrition. *Adv. Food Nutr. Res.* **40:** 3–24.
15. Lewis, K. C., M. H. Green, J. B. Green, and L. A. Zech. 1990. Retinol metabolism in rats with low vitamin A status: a compartmental model. *J. Lipid Res.* **31:** 1535–1548.
16. Kelley, S. K., C. B. Nilsson, M. H. Green, J. B. Green, and H. Håkansson. 1998. Use of model-based compartmental analysis to study effects of 2,3,7,8-tetrachlorodibenzo-p-dioxin on vitamin A kinetics in rats. *Toxicol. Sci.* **44:** 1–13.
17. Green, M. H., and J. B. Green. 2003. The use of model-based compartmental analysis to study vitamin A metabolism in a non-steady state. *Adv. Exp. Med. Biol.* **537:** 159–172.
18. Lewis, K. C., M. H. Green, and B. A. Underwood. 1981. Vitamin A turnover in rats as influenced by vitamin A status. *J. Nutr.* **111:** 1135–1144.
19. Green, M. H., J. B. Green, and K. C. Lewis. 1987. Variation in retinol utilization rate with vitamin A status in the rat. *J. Nutr.* **117:** 694–703.
20. Jang, J. T., J. B. Green, J. L. Beard, and M. H. Green. 2000. Kinetic analysis shows that iron deficiency decreases liver vitamin A mobilization in rats. *J. Nutr.* **130:** 1291–1296.
21. Smith, J. E., D. C. Lawless, M. H. Green, and R. C. Moon. 1992. Secretion of vitamin A and retinol-binding protein into plasma is depressed in rats by N-(4-hydroxyphenyl)retinamide (fenretinide). *J. Nutr.* **122:** 1999–2009.
22. Kelley, S. K., C. B. Nilsson, M. H. Green, J. B. Green, and H. Håkansson. 2000. Mobilization of vitamin A stores in rats after administration of 2,3,7,8-tetrachlorodibenzo-p-dioxin: a kinetic analysis. *Toxicol. Sci.* **55:** 478–484.
23. Green, M. H., and J. B. Green. 1994. Vitamin A intake and status influence retinol balance, utilization and dynamics in rats. *J. Nutr.* **124:** 2477–2485.
24. Reeves, P. G., F. H. Nielsen, and G. C. Fahey, Jr. 1993. AIN-93 purified diets for laboratory rodents: final report of the American Institute of Nutrition ad hoc writing committee on the reformulation of the AIN-76A rodent diet. *J. Nutr.* **123:** 1939–1951.
25. Green, M. H., R. W. Snyder, S. A. Akohoue, and J. B. Green. 2001. Increased rat mammary tissue vitamin A associated with increased vitamin A intake during lactation is maintained after lactation. *J. Nutr.* **131:** 1544–1547.
26. Stefanovski, D., P. J. Moate, and R. C. Boston. 2003. WinSAAM: a Windows-based compartmental modeling system. *Metabolism.* **52:** 1153–1166.
27. Wang, L. 1959. Plasma volume, cell volume, total blood volume and F_{cells} factor in the normal and splenectomized Sherman rat. *Am. J. Physiol.* **196:** 188–192.

28. Furr, H. C., M. H. Green, M. Haskell, N. Mokhtar, P. Nestel, S. Newton, J. D. Ribaya-Mercado, G. Tang, S. Tanumihardjo, and E. Wasantwisut. 2005. Stable isotope dilution techniques for assessing vitamin A status and bioefficacy of provitamin A carotenoids in humans. *Public Health Nutr.* **8:** 596–607.
29. Akaike, H. 1974. A new look at the Statistical Model Identification. *IEEE Trans. Automat. Control.* **19:** 716–723.
30. Green, M. H., J. B. Green, T. Berg, K. R. Norum, and R. Blomhoff. 1993. Vitamin A metabolism in rat liver: a kinetic model. *Am. J. Physiol.* **264:** G509–G521.
31. Ramsden, D. B., H. P. Prince, W. A. Burr, A. R. Bradwell, E. G. Black, A. E. Evans, and R. Hoffenberg. 1978. The inter-relationship of thyroid hormones, vitamin A and their binding proteins following acute stress. *Clin. Endocrinol. (Oxf.).* **8:** 109–122.
32. Mitra, A. K., M. A. Wahed, A. K. Chowdhury, and C. B. Stephensen. 2002. Urinary retinol excretion in children with acute watery diarrhoea. *J. Health Popul. Nutr.* **20:** 12–17.
33. Sijtsma, S. R., C. E. West, J. H. Rombout, and A. J. Van der Zijpp. 1989. Effect of Newcastle disease virus infection on vitamin A metabolism in chickens. *J. Nutr.* **119:** 940–947.
34. Takase, S., T. Goda, H. Yokogoshi, and T. Hoshi. 1991. Effects of various dietary protein contents on vitamin A status of rats exposed to prolonged immobilization through suspension. *J. Nutr. Sci. Vitaminol. (Tokyo).* **37:** 443–452.
35. Felding, P., and G. Fex. 1985. Rates of synthesis of prealbumin and retinol-binding protein during acute inflammation in the rat. *Acta Physiol. Scand.* **123:** 477–483.
36. West, C. E., S. R. Sijtsma, B. Kouwenhoven, J. H. Rombout, and A. J. van der Zijpp. 1992. Epithelia-damaging virus infections affect vitamin A status in chickens. *J. Nutr.* **122:** 333–339.
37. Kanda, Y., N. Yamamoto, and Y. Yoshino. 1990. Utilization of vitamin A in rats with inflammation. *Biochim. Biophys. Acta.* **1034:** 337–341.
38. Dominguez Fernandez, E., S. Flohe, F. Siemers, M. Nau, and F. U. Schade. 2002. Endotoxin tolerance in rats: influence on LPS-induced changes in excretory liver function. *Inflamm. Res.* **51:** 500–505.
39. Neuzil, K. M., W. C. Gruber, F. Chytil, M. T. Stahlman, B. Engelhardt, and B. S. Graham. 1994. Serum vitamin A levels in respiratory syncytial virus infection. *J. Pediatr.* **124:** 433–436.
40. Rosales, F. J., C. Kjolhede, and S. Goodman. 1996. Efficacy of a single oral dose of 200,000 IU of oil-soluble vitamin A in measles-associated morbidity. *Am. J. Epidemiol.* **143:** 413–422.
41. Tomkins, A. 2003. Assessing micronutrient status in the presence of inflammation. *J. Nutr.* **133 (Suppl.):** 1649–1655.